

Nonlinear combining of laser beams

Pavel M. Lushnikov* and Natalia Vladimirova

Department of Mathematics and Statistics, University of New Mexico, New Mexico 87131, USA

*Corresponding author: plushnik@math.unm.edu

Received April 7, 2014; accepted April 28, 2014;
posted May 2, 2014 (Doc. ID 209631); published June 4, 2014

We propose to combine multiple laser beams into a single diffraction-limited beam by beam self-focusing (collapse) in a Kerr medium. Beams with total power above critical are first combined in the near field and then propagated in the optical fiber/waveguide with Kerr nonlinearity. Random fluctuations during propagation eventually trigger a strong self-focusing event and produce a diffraction-limited beam carrying the critical power. © 2014 Optical Society of America

OCIS codes: (190.0190) Nonlinear optics; (260.5950) Self-focusing; (190.4370) Nonlinear optics, fibers; (140.3510) Lasers, fiber.

<http://dx.doi.org/10.1364/OL.39.003429>

A dramatic rise of the output power of fiber lasers in the last 25 years [1,2] resulted in reaching 10 kW in 2009 [3] for the diffraction-limited beam. Also 20 kW continuous-wave commercial fiber laser was announced in 2013 [4], although the beam quality is not yet specified. However, the growth of power since 2009 has been mostly stagnated because of the encountered mode instabilities [2]. A further increase of the total power of the diffraction-limited beam is possible through coherent beam combining [1,5] where the phase of each laser beam is controlled to ideally produce the combined beam with the coherent phase. Beam combining has been successfully demonstrated only for several beams, e.g., [6] achieved the combining of five 500 W laser beam into a 1.9 kW Gaussian beam with good beam quality $M^2 = 1.1$. Nonlinearity is expected to be the key issue for further scaling of coherent beam combining [1].

Here we propose to use nonlinearity to our advantage to achieve combining multiple laser beams into a diffraction-limited beam by strong self-focusing in a waveguide with Kerr nonlinearity. The number of laser beams can be arbitrary, but we require the total power to exceed the critical power of self-focusing. Our estimates below suggest that the commercially available fiber of 1 mm diameter [4] might be a possible choice of waveguide to achieve the diffraction limited beam with the power of several MWs.

We first consider stationary self-focusing of the laser beam in the Kerr medium, assuming for now that the pulse duration is long enough to neglect time-dependent effects. (We estimate the range of allowed pulse durations below.) The propagation of a quasi-monochromatic beam with a single polarization through the Kerr media is described by the nonlinear Schrödinger equation (NLSE) (see, e.g., [7]):

$$i\partial_z\psi + \frac{1}{2k}\nabla^2\psi + \frac{kn_2}{n_0}|\psi|^2\psi = 0, \quad (1)$$

where the beam is directed along the z axis, $\mathbf{r} \equiv (x, y)$ are the transverse coordinates, $\psi(\mathbf{r}, z)$ is the envelope of the electric field, $\nabla \equiv ((\partial/\partial x), (\partial/\partial y))$, $k = 2\pi n_0/\lambda_0$ is the wavenumber in media, λ_0 is the vacuum wavelength, n_0 is the linear index of refraction, and n_2 is the nonlinear Kerr index. The index of refraction is $n = n_0 + n_2I$,

where $I = |\psi|^2$ is the light intensity. In fused silica $n_0 = 1.4535$, $n_2 = 3.2 \cdot 10^{-16} \text{ cm}^2/\text{W}$ for $\lambda_0 = 790 \text{ nm}$ and $n_0 = 1.4496$, $n_2 = 2.46 \cdot 10^{-16} \text{ cm}^2/\text{W}$ for $\lambda_0 = 1070 \text{ nm}$.

The NLSE in Eq. (1) is converted into the dimensionless form,

$$i\partial_z\psi + \nabla^2\psi + |\psi|^2\psi = 0, \quad (2)$$

by the scaling transformation $(x, y) \rightarrow (x, y)w_0$, $z \rightarrow 2zkw_0^2$, and $\psi \rightarrow \psi n_0^{1/2}/(2k^2w_0^2n_2)^{1/2}$, where w_0 is of the order of the order of the waists of each combined laser beam.

NLSE in Eq. (1) describes the catastrophic self-focusing (collapse) [8,9] of the laser beam provided the power P exceeds the critical value of

$$P_c = \frac{N_c\lambda_0^2}{8\pi^2n_2n_0} \simeq \frac{11.70\lambda_0^2}{8\pi^2n_2n_0}. \quad (3)$$

Here $N_c \equiv 2\pi \int R^2 r dr = 11.7008965\dots$ is the critical power for the NLSE in Eq. (2) in dimensionless units, and $R(r)$ is the radially symmetric Townes soliton [10] defined as the ground-state soliton $\psi = e^{iz}R(r)$ of NLSE with $-R + \nabla^2R + R^3 = 0$, where $r \equiv |\mathbf{r}|$. In fused silica $P_c \simeq 2 \text{ MW}$ for $\lambda_0 = 790 \text{ nm}$ and $P_c \simeq 4.7 \text{ MW}$ for $\lambda_0 = 1070 \text{ nm}$. In air $P_c \simeq 2.4 \text{ GW}$ for $\lambda_0 = 790 \text{ nm}$.

Assume that N laser beams are combined in the near field (side-by-side combining) at the entrance $z = 0$ to the optical waveguide (the optical fiber) as shown in Fig. 1. The waveguide can be either multimode optical fiber or any type of waveguide structure with the Kerr nonlinearity (e.g., it can be a capillar with the reflective

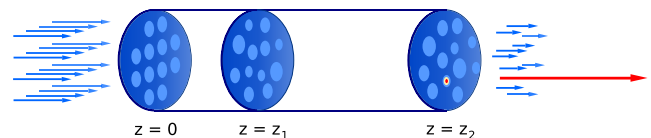


Fig. 1. Schematic of nonlinear beam combining. An array of beams with noncorrelated phases enters a nonlinear optical fiber at $z = 0$. Inside the fiber, the laser field is randomized due to nonlinear interactions (as shown for a typical cross section at $z = z_1$). A large fluctuation of that random field triggers a strong self-focusing event producing a nearly diffraction-limited hot spot at $z = z_2$ (shown by the long arrow), which carries the critical power P_c .

internal walls, filled by a gas or a liquid with the dominated Kerr nonlinearity). We assume that the diameter of waveguide is large enough for the applicability of the NLSE in Eq. (2). The single polarization is ensured, e.g., by the use of the polarization-maintaining optical fiber. We note that a generalization to a case of arbitrary polarization is possible but is beyond the scope of this Letter.

The properties of the waveguide in our simulations are taken into account through the boundary conditions in the NLSE along x and y . An example is the multi-mode optical fiber with the diameter in the range between hundreds of μm to several mm. At $z = 0$, we approximate each beam to have the Gaussian form with the plane wavefront so that the initial condition for the NLSE in Eq. (2) is the superposition of these Gaussians $\psi(x, y)|_{z=0} = \sum_{n=1}^N \psi_n$, $\psi_n = A_n \exp(-((x - x_n)^2 + (y - y_n)^2)/r_n^2 + i\phi_n)$, where r_n, A_n, ϕ_n and (x_n, y_n) are the width, amplitude, phase, and location of the center of the n th beam, respectively. In simulation, we assume the same amplitudes $A = A_n$ and widths $r_n = r_0$ for all N beams, but phases ϕ_n are randomly distributed at $[0, 2\pi]$. Randomness of phases ϕ_n reflects the randomness in environmental fluctuations and fiber amplifiers of lasers.

Figure 2 shows the NLSE in Eq. (2) simulation for a square array of $N = 10 \times 10$ beams at $z = 0$, which is uniformly located in $0 < x < L, 0 < y < L, L = 25.6$ with periodic boundary conditions in x and y . Each beam had a radius of $r_0 = 1.13$ and carried the power $0.1P_c$ (the total power is $10P_c$).

The middle column of Fig. 2 ($z = z_1$) shows that the amplitudes and phases become random after propagation of the nonlinear distance $z_{\text{nl}} \equiv 1/\langle |\psi|^2 \rangle$, where $\langle |\psi|^2 \rangle = P/S$ is the spatial average of the light intensity in the cross-section area S at $z = \text{const}$. For $z > z_{\text{nl}}$ the amplitude and phase experience fluctuations along z (optical turbulence) until a large fluctuation at $z \simeq 15$ triggers a strong self-focusing event, which results in the formation of a large amplitude near-diffraction-limited beam (right column of Fig. 2 shown for $z = z_2$). These simulations were performed 360 times for initial conditions with different randomly selected phases of the input beams. The probability density function (PDF) of the distance z_{sf} along the fiber to the point of the first catastrophic self-focusing event are shown in

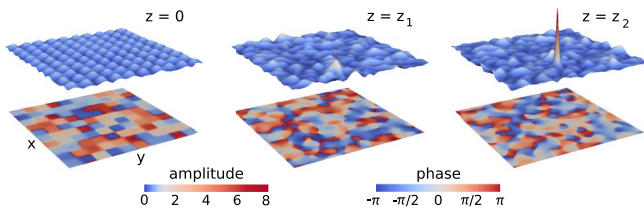


Fig. 2. Simulation of nonlinear beam combining in NLSE in Eq. (2). The snapshots of the distributions (vertical axis) in (x, y) of the amplitude $|\psi|$ (top row) and the phase $\arg(\psi)$ (bottom row) for different values of z . Left column: array of Gaussian beams with random phases are used as initial conditions ($z = 0$). Middle column: Kerr nonlinearity results in randomization of phases and amplitudes after the propagation distance $z \sim z_{\text{nl}}$, as shown for $z = z_1 = 10$ ($z_{\text{nl}} = 5.6$ in that case). Right column: random fluctuations of amplitudes trigger the strong self-focusing collapse event ($z = z_2 = 15$).

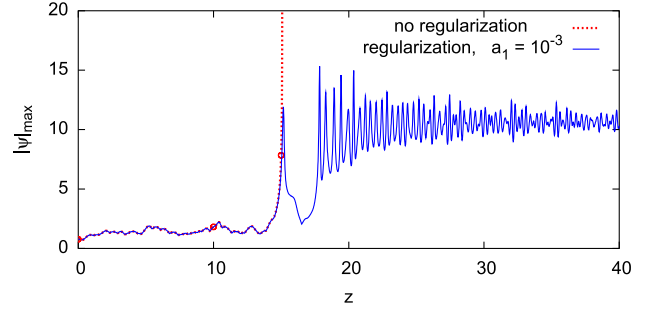


Fig. 3. $\max_{(x,y)} |\psi|$ in the waveguide's cross section versus z . Dashed line shows the result of the same simulation of the NLSE in Eq. (2) as in Fig. 2. The solid line shows the simulation of the regularized NLSE in Eq. (5) with $a_1 = 0.001$ and the same initial condition as for the dashed curve. Thick dots correspond to $z = z_1$ and $z = z_2$ of Fig. 2.

Figs. 4(a) and 4(b) for 10×10 and 8×8 beams, respectively. The power in each beam for these two cases is $0.1P_c$ and $0.156P_c$, respectively. The average value $\langle z_{\text{sf}} \rangle$ (averaged over the ensemble of these 360 simulations) and the standard deviation $\langle \delta z_{\text{sf}} \rangle \equiv (\langle z_{\text{sf}}^2 \rangle - \langle z_{\text{sf}} \rangle^2)^{1/2}$ are $\langle z_{\text{sf}} \rangle = 31.30$, $\langle \delta z_{\text{sf}} \rangle = 16.87$ and $\langle z_{\text{sf}} \rangle = 12.55$, $\langle \delta z_{\text{sf}} \rangle = 6.86$ for the simulations of Figs. 4(a) and 4(b), respectively. 8×8 beams with $0.125P_c$ give $\langle z_{\text{sf}} \rangle = 26.62$ and $\langle \delta z_{\text{sf}} \rangle = 14.39$. We also performed simulations with the added linear potential (circular barrier at $r = 0.45L$) in Eq. (2) to model the boundary of the waveguide in transverse directions (x, y) and obtained similar results for PDF (a type of boundary condition is typically essential only for $z < z_{\text{nl}}$, provided the barrier is high enough to make the escape of light from the waveguide a small correction which simulates the total internal reflection). The typical result of such simulations is shown in Fig. 5.

The high-amplitude beam (the collapsing filament), as in the right row of Fig. 2, is well approximated by the rescaled Townes soliton [10]:

$$|\psi(x, y, z)| \simeq L(z)^{-1} R(\rho), \quad \rho \equiv r/L(z), \quad |\mathbf{r}| \equiv r, \quad (4)$$

where $L(z)$ is the z -dependent beam width. The detailed explicit form of $L(z)$ dependence was found in [11] starting from the amplitude $|\psi|$ about three to four times above the initial value. Thus the collapsing beam of Fig. 2 approaches diffraction-limited beam of the form in Eq. (4) as it grows only three to four times above the background value $\langle |\psi|^2 \rangle^{1/2}$. This is also consistent with the study of the optical turbulence dominated by collapses [12–15] that the collapses are well defined as their

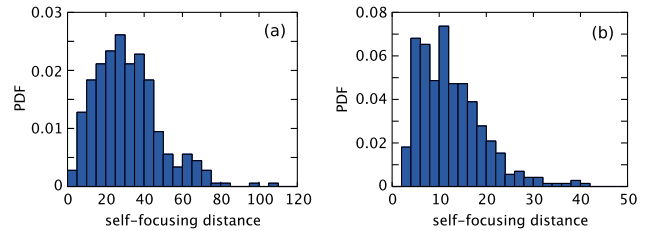


Fig. 4. Probability density functions (PDFs) of the catastrophic self-focusing distance z_{sf} collected over 360 simulations with random initial phases and the total power $10P_c$. (a) $N = 10 \times 10$ combined beams with $r_0 = 1.13$. (b) $N = 8 \times 8$ combined beams with $r_0 = 1.41$.

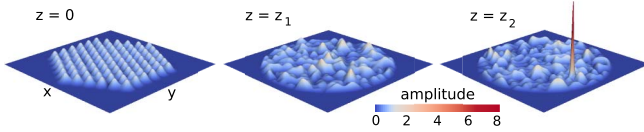


Fig. 5. Simulation similar to Fig. 2 with 91 beams of the power $0.1P_c$ and $r_0 = 1.13$, but with the added circular barrier at $r = 0.45L$ to represent the total internal reflection of the circular waveguide. $z_1 = 1$ and $z_2 = 9.7$.

amplitudes exceed the background values three to four times.

We also note that for $z > z_{nl}$ (i.e., after the initial transient propagation), the fluctuations of the intensity $|\psi|^2$ about $\langle |\psi|^2 \rangle$ have the universal form determined by $\langle |\psi|^2 \rangle$ and r_0 [14,15]. It means that the launching of beams (at $z = 0$) with $P > P_c$ into a waveguide unavoidably results in the catastrophic collapse for large enough distance z_{sf} if we neglect the waveguide's linear losses as assumed in the NLSE in Eq. (1). The decrease of the total power closer to P_c only increases z_{sf} (but the value of z_{sf} always remain finite). Also for very large z_{sf} , one can compensate linear losses by the additional periodical (along z) coupling of the waveguide with the external pump.

The regularization of the catastrophic self-focusing depends on the particular type of the Kerr medium. One type of the regularization is the addition of the saturating nonlinearity into NLSE in Eq. (2) as follows:

$$i\partial_z\psi + \nabla^2\psi + |\psi|^2\psi - a_1|\psi|^4\psi = 0, \quad (5)$$

where $0 < a_1 \ll 1$. This type of saturated nonlinearity was found, e.g., in chalcogenide glasses with the negative fifth order nonlinearity $n = n_0 + n_2I + n_4I^2$, $n_4 < 0$ [16]. The dashed line in Fig. 3 shows the z dependence of the maximum amplitude $\max_{(x,y)}|\psi|$ for the solution of Eq. (5) with $a_1 = 0.001$ and the same initial condition as for the solid curve of Fig. 3. It is seen that instead of the catastrophic collapse near $z_2 = 20$ as in the NLSE in Eq. (2), we observe the periodic oscillations with the maximum amplitude roughly estimated as $|\psi| \simeq 1/a_1^{1/3}$.

Another type of the collapse regularization is the multiphoton absorption described by the term $i(\beta^{(K)}/2)|\psi|^{2K-2}\psi$ added to the left-hand side (l.h.s.) of the NLSE in Eq. (1). Here K is the number of photons absorbed by the electron in each elementary process (K photon absorption) and $\beta^{(K)}$ is the multiphoton absorption coefficient. For fused silica with $\lambda_0 = 790$ nm, a dominated nonlinear absorption process for this wavelength is $K = 5$ with $\beta^{(5)} = 1.80 \cdot 10^{-51} \text{ cm}^7 \text{ W}^{-4}$ [7], which leads to the formation of plasma and optical damage.

Special measures must be taken to prevent the damage of the waveguide. A detailed discussion of that topic is outside the scope of this Letter, and we only highlight below possible ways to overcome that difficulty. The first and perhaps simplest way is to use a waveguide short enough to avoid a full development of the catastrophic collapse. An obvious drawback would be that only a fraction of the initial distribution of phases would result in strong self-focusing producing a near-diffraction-limited beam. The second possible choice is to use a waveguide

filled with gas and ultrashort pulses such that the multiphoton ionization produces plasma, which results in the plasma defocusing and clamping of the collapsing filament. Such type of clamping has been demonstrated experimentally to allow a formation of filaments of up to several meters in length [7,17] for the propagation of ultrashort pulses in air. The drawback of that approach is that it would allow beam combining to short pulses only limiting the total energy of the combined beam. The third option is to use chalcogenide glasses with the negative fifth order nonlinearity as described in Eq. (5) [16]. The fourth choice is to use a waveguide with the specially chosen transverse profile of $n_0(x,y)$ and $n_2(x,y)$ such that the collapse starts near the center of the waveguide because of the larger value of n_0 there, while the catastrophic collapse is stopped by the decrease of n_2 is that region [18]. The fifth choice is nonlinearity management [19] when n_2 is periodically modulated along z to prevent the collapse. The sixth choice is to form a ring cavity from the waveguide such that the length of the single round trip along the cavity (i.e., along z) is not sufficient to achieve catastrophic collapse while the optical switching is used to remove from the cavity the nearly collapsed diffraction-limited beam. A power depletion from such removal can be compensated by the coupling of the cavity to the laser beams.

To estimate parameters for a potential experimental realization, we assume that the typical intensity from the combined beams in the waveguide is $I_0 = 10^9 \text{ W/cm}^2$, which allows continuous-wave (cw) operation without optical damage [20]. Assume $\langle z_{sf} \rangle = 31.30$ for 10×10 combined beams as in Fig. 4(a). Using the parameters $n_0 = 1.4496$, and $n_2 = 2.46 \cdot 10^{-16} \text{ cm}^2/\text{W}$ of fused silica at $\lambda_0 = 1070$ nm (corresponding to the wavelength of the commercially available 50 kW cw fiber laser [4]), we obtain in dimensional units the typical required length of the waveguide $l \sim \langle z_{sf} \rangle = 4$ m and the waveguide thickness 2 mm, which is comparable with the commercially available fiber of 1 mm diameter [4]. Thus we estimate that combining several hundred beams from 50 kW cw fiber laser [4] may allow us to produce a nearly diffraction-limited combined beam with the power $\simeq P_c = 4.7$ MW. We also note that the high beam quality is not required for each of the combining beams because the self-focusing collapse spontaneously produces the near diffraction-limited beam from the generic superpositions of combined beams.

For the pulsed operations, the optical damage threshold is higher than for cw, which would allow us to achieve nonlinear beam combining in a smaller settings, e.g., typical experimental measurements of the optical damage threshold in fused silica give the threshold intensity $I_{\text{thresh}} \sim 5 \cdot 10^{11} \text{ W/cm}^2$ for 8 ns pulses and $I_{\text{thresh}} \sim 1.5 \cdot 10^{12} \text{ W/cm}^2$ for 14 ps pulses [21]. Thus the short pulse operations might allow us to scale down the typical lengths l in z and the waveguide cross section in 2–3 orders of magnitude for the same optical power. However, for such short pulse durations, t_0 , we generally might need to take into account a group velocity dispersion (GVD). Its contribution is described by the addition of the term $-(\beta_2/2)(\partial^2/\partial t^2)\psi$ into the left-hand side of Eq. (1). Here $\beta_2 = 370 \text{ fs}^2/\text{cm}$ is the GVD coefficient for fused silica at $\lambda_0 = 790$ nm, and t is the retarded time

$t \equiv T - z/c$, where T is the physical time and c is the speed of light. At fiber lengths in several meters, the linear absorption of optical grade fused silica is still negligible. The GVD distance $\tilde{z}_{\text{GVD}} \equiv 2t_0^2/\beta_2$ must exceed l for the NLSE applicability, which gives $t_0 \gtrsim 0.3$ ps for $l = 4$ m.

Another possible effect beyond NLSE includes stimulated Brillouin scattering (can be neglected for the pulse duration $\lesssim 10$ ns [22], or, similar, if the linewidth of the lasers is made large enough) and a stimulated Raman scattering (SRS). The threshold of SRS for a long pulse in fused silica was estimated from a gain exponent $gI_0l \simeq 16$, where $g \simeq 10^{-11}$ cm/W is the Raman gain constant [22]. This estimate was obtained assuming that the spontaneous emission is amplified by SRS (with the amplification factor $e^{gI_0l} = e^{16}$) up to the level of the average light intensity I_0 in the waveguide. Taking $l = 4$ m and $I_0 = 10^9$ W/cm², we obtain the gain exponent $gI_0l \simeq 4 \ll 16$, i.e., we still operate well below the SRS threshold and can neglect SRS. This SRS threshold estimate is true for relatively long pulses $\gtrsim 10$ ps [22]. For pulses of shorter duration, SRS is additionally suppressed because the laser beam and the SRS wave move with different group velocities.

In conclusion, we demonstrated the possibility to achieve nonlinear beam combining by propagating multiple laser beams in the waveguide with the Kerr nonlinearity. Large fluctuations during propagation seed the collapse event resulting in the formation of a near-diffraction-limited beam.

A part of this work was done during N. V.'s visit to the Kalvi Institute for Theoretical Physics, UCSB, supported by grant no. NSF PHY11-25915. Simulations were performed at the Center for Advanced Research Computing, UNM.

References

1. D. J. Richardson, J. Nilsson, and W. A. Clarkson, *J. Opt. Soc. Am. B* **27**, B63 (2010).
2. C. Jauregui, J. Limpert, and A. Tünnermann, *Nat. Photonics* **7**, 861 (2013).
3. V. Gapontsev, F. A. Fomin, and M. Abramov, in *Proceedings of Advanced Solid-State Photonics* (Optical Society of America, 2010), paper AWA1.
4. <http://www.ipgphotonics.com>.
5. T. Y. Fan, *IEEE J. Sel. Top. Quantum Electron.* **11**, 567 (2005).
6. S. M. Redmond, D. J. Ripin, C. X. Yu, S. J. Augst, T. Y. Fan, P. A. Thielen, J. E. Rothenberg, and G. D. Goodno, *Opt. Lett.* **37**, 2832 (2012).
7. L. Bergé, S. Skupin, R. Nuter, J. Kasparian, and J.-P. Wolf, *Rep. Prog. Phys.* **70**, 1633 (2007).
8. S. N. Vlasov, V. A. Petrishchev, and V. I. Talanov, *Izv. Vyssh. Uchebn. Zaved., Radiofiz.* **14**, 1353 (1971).
9. V. E. Zakharov, *Sov. Phys. JETP* **35**, 908 (1972).
10. C. Sulem and P. L. Sulem, *Nonlinear Schrödinger Equations: Self-Focusing and Wave Collapse* (World Scientific, 1999).
11. P. M. Lushnikov, S. A. Dyachenko, and N. Vladimirova, *Phys. Rev. A* **88**, 013845 (2013).
12. P. M. Lushnikov and H. A. Rose, *Phys. Rev. Lett.* **92**, 255003 (2004).
13. P. M. Lushnikov and H. A. Rose, *Plasma Phys. Controlled Fusion* **48**, 1501 (2006).
14. P. M. Lushnikov and N. Vladimirova, *Opt. Lett.* **35**, 1965 (2010).
15. Y. Chung and P. M. Lushnikov, *Phys. Rev. E* **84**, 036602 (2011).
16. G. Boudebs, S. Cherukulappurath, H. Leblond, J. Troles, F. Smektala, and F. Sanchez, *Opt. Commun.* **219**, 427 (2003).
17. O. Kosareva, J.-F. Daigle, N. Panov, T. Wang, S. Hosseini, S. Yuan, G. Roy, V. Makarov, and S. L. Chin, *Opt. Lett.* **36**, 1035 (2011).
18. S. K. Turitsyn, Aston University, Birmingham, UK (private communication, 2012).
19. I. R. Gabitov and P. M. Lushnikov, *Opt. Lett.* **27**, 113 (2002).
20. J. W. Dawson, M. J. Messerly, R. J. Beach, M. Y. Shverdin, E. A. Stappaerts, A. K. Sridharan, P. H. Pax, J. E. Heebner, C. W. Siders, and C. Barty, *Opt. Commun.* **16**, 13240 (2008).
21. A. V. Smith and B. T. Do, *Appl. Opt.* **47**, 4812 (2008).
22. G. Agrawal, *Nonlinear Fiber Optics*, 5th ed. (Academic, 2012).